

An Analysis of Sampling Effect on Bilateral Teleoperation System Transparency

Ting YANG^{1,2}, Yi Li FU^{1,*}, Mahdi TAVAKOLI²

1. State Key Laboratory of Robotics and Systems, Harbin Institute of Technology, Harbin, Heilongjiang, 150080, China
 E-mail: yangtinghit@gmail.com, ylfms@hit.edu.cn

2. Department of Electrical and Computer Engineering, University of Alberta, Edmonton, Alberta, T6G 2V4 Canada
 E-mail: mahdi.tavakoli@ualberta.ca

Abstract: The performances of continuous-time controlled and discrete-time controlled bilateral teleoperation systems are mathematically and experimentally studied and compared. The results show that under stability conditions, continuous-time controlled teleoperation systems have hybrid matrix parameters that are closer to their ideal values than their discrete-time controlled counterparts. This means better force tracking and position tracking performance under continuous-time control, which can lead to better task performance.

Key Words: Bilateral teleoperation, hybrid parameters, discrete-time control, continuous-time control, system performance

1 Introduction

In a bilateral teleoperation system, a human operator manipulates and receives force feedback from an environment through a “teleoperator”, which consists of the master robot, the communication channel, the controllers, and the slave robot [1]. While stability is a primary requisite for safe teleoperation, the performance (transparency) of the teleoperator determines whether the human operator can accomplish given tasks in the teleoperation mode.

The performance of a teleoperator can be judged based on the transmitted impedance to the human operator – this should be as close as possible to the slave’s environment impedance. The position tracking performance and force tracking performance of the system between the master and the slave are also measures of teleoperator transparency [2-4]. After modelling a teleoperator, its hybrid matrix can be derived, which can be analyzed to evaluate the teleoperator’s performance.

In this paper, by comparing the hybrid parameters of continuous-time controlled and discrete-time controlled bilateral teleoperation systems under stability conditions, we show that better system performance can be obtained with a continuous-time controller.

2 Formatting Instructions

A continuous-time position-error-based (PEB) teleoperation system is shown in Fig. 1. In this paper, the PEB teleoperation control method is chosen because, for direct force reflection (DFR) control, even a continuous-time controlled teleoperation system will not be absolutely stable [3].

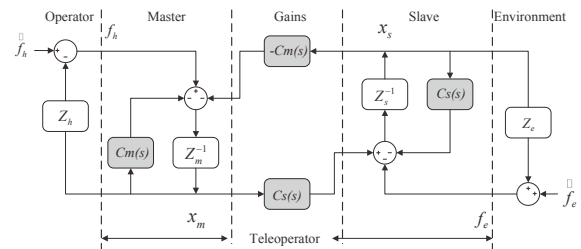


Fig. 1: A continuous-time two-channel bilateral teleoperation system. The shaded blocks represent controllers.

Here, f_h is the interaction force between the master robot and the human operator, and f_e is the interaction force between the slave robot and the environment. Also, \tilde{f}_h and \tilde{f}_e represent the exogenous human operator and environment forces, respectively. x_m and x_s denote the positions of the master and slave, respectively. Z_h , Z_e , Z_m and Z_s are the impedances of the operator, the environment, the master robot, and the slave robot, respectively. The proportional-derivative (PD) position controllers $C_m = k_{v_m}s + k_{p_m}$ and $C_s = k_{v_s}s + k_{p_s}$ are typically used for the master robot and the slave robot, respectively.

The dynamics of the operator and the environment are

$$\begin{aligned} \tilde{F}_h - F_h &= Z_h(s)sX_m, \\ \tilde{F}_e - F_e &= Z_e(s)sX_s, \end{aligned} \quad (1)$$

where s is the Laplace operator. The teleoperator can be modelled as a two-port network with the hybrid matrix representation

$$\begin{bmatrix} F_h(s) \\ -sX_s(s) \end{bmatrix} = H(s) \begin{bmatrix} sX_m(s) \\ F_e(s) \end{bmatrix}, \quad (2)$$

where the hybrid matrix $H(s)$ is

$$H(s) = \begin{bmatrix} h_{11} & h_{12} \\ h_{21} & h_{22} \end{bmatrix}. \quad (3)$$

* Corresponding author.

This research is supported by the Natural Sciences and Engineering Research Council (NSERC) of Canada, by the Canada Foundation for Innovation (CFI), by Self-Planned Task (NO.SKLR201403B) of State Key Laboratory of Robotics and System (HIT) and by the China Scholarship Council (CSC) under grant [2013]06120200.

Each element of the H matrix has a physical meaning. The hybrid parameter $h_{11} = F_h/sX_m|_{F_e=0}$ is the input impedance felt by the operator in the free-motion condition. The parameter $h_{12} = F_h/F_e|_{sX_m=0}$ is a measure of force tracking in the haptic teleoperation system when the master is locked in motion. The parameter $h_{21} = -X_s/X_m|_{F_e=0}$ is a measure of the position (velocity) tracking performance when the slave is in free space. The parameter $h_{22} = -sX_s/F_e|_{sX_m=0}$ is the output admittance when the master is locked in motion.

Thus the hybrid matrix for Fig. 1 is given as

$$H = \begin{bmatrix} Z_m + C_m \frac{Z_s}{Z_s + C_m} & \frac{C_m}{Z_s + C_m} \\ -\frac{C_s}{Z_s + C_s} & \frac{1}{Z_s + C_s} \end{bmatrix}. \quad (4)$$

For ideal transparency, the hybrid matrix in (4) should be

$$H_{ideal} = \begin{bmatrix} 0 & 1 \\ -1 & 0 \end{bmatrix} \quad (5)$$

Nonzero values for h_{11} mean that even when the slave is in free space, the user will receive some force feedback. Nonzero values for h_{22} mean that when the master is locked in place, the slave will move in reaction to slave/environment contacts. Deviations from 1 and -1 for h_{12} and h_{21} indicate imperfect force tracking and position tracking between the master and slave robots, respectively.

In this paper, by comparing the hybrid matrix elements in continuous-time teleoperation systems with discrete-time teleoperation systems, the advantages of continuous-time control of bilateral teleoperation systems will be revealed.

3 Modelling of a teleoperation system with discrete-time bilateral control

The two-channel PEB teleoperation system of Fig. 1 under discrete-time control is shown in Fig. 2. As shown, the operator, the master, the slave and the environment remain continuous-time entities. However, the controllers will be replaced by their discrete-time counterparts.

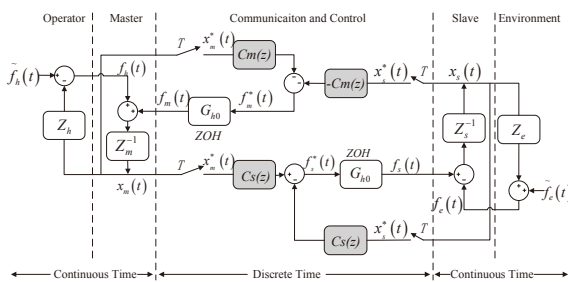


Fig. 2: Digitally controlled two-channel bilateral teleoperation system. The shaded blocks represent controllers.

For an input $f(t)$ to an ideal sampler starting at $t = 0$, the output is $f^*(t) = \sum_{k=0}^{\infty} f(kT)\delta(t - kT)$ where T is the sampling period. Since $z = e^{sT}$, the Laplace and Z transforms of the sampled-data signal $f^*(t)$ are

$$F^*(s) = L[f^*(t)] = \sum_{k=0}^{\infty} f(kT)e^{-kTs} \quad \text{and}$$

$F(z) = Z[f^*(t)] = F^*(s)|_{s=(1/T)\ln z}$, respectively. In Fig. 2, the two zero-order hold (ZOH) blocks reconstruct continuous-time control signals $f_m(t)$ and $f_s(t)$ from discrete-time counterparts $f_m^*(t)$ and $f_s^*(t)$ via the following transfer function:

$$G_{h0}(s) = \frac{1 - e^{-Ts}}{s} \quad (6)$$

In Fig. 2, since $C_m(z)$ and $C_s(z)$ are both discrete-time controllers, the discrete time control signals for the master and the slave can be written as

$$\begin{aligned} F_m^* &= -C_m(z)(X_m^* + X_s^*) \\ F_s^* &= C_s(z)(X_m^* - X_s^*) \end{aligned} \quad (7)$$

Using (7) and substituting $F_m = G_{h0}F_m^*$ and $F_s = G_{h0}F_s^*$ in (2), the closed-loop dynamics of the master and the slave in discrete-time are written as

$$\begin{aligned} X_m(z) &= Z[Z_m^{-1}F_h] + Z[Z_m^{-1}G_{h0}] \cdot \\ &\quad (-C_m(z)X_m(z) + C_m(z)X_s(z)) \\ X_s(z) &= -Z[Z_s^{-1}F_e] + Z[Z_s^{-1}G_{h0}] \cdot \\ &\quad (C_s(z)X_m(z) - C_s(z)X_s(z)) \end{aligned} \quad (8)$$

With $Z_m = M_m s^2$ and $Z_s = M_s s^2$, where M_m and M_s are the master and the slave inertias, respectively, we have

$$Z[Z_{m,s}^{-1}G_{h0}] = \frac{T^2}{2M_{m,s}} \frac{z+1}{(z-1)^2} \quad (9)$$

For brevity, commas in subscripts mean 'or' and present multiple equations. Using Tustin's method, the PD controller C_s is discretized as $C_s(z) = k_{v_s} (2(z-1)/(T(z+1))) + k_{p_s}$ and here we choose $C_m = C_s$.

Note that in (8), $Z[Z_m^{-1}F_h] \neq Z_m^{-1}(z)F_h(z)$ and $Z[Z_s^{-1}F_e] \neq Z_s^{-1}(z)F_e(z)$ because the master and the slave transfer functions Z_m^{-1} and Z_s^{-1} operate in continuous time (i.e., F_h and F_e are not sampled). To be able to derive a hybrid model representation from (6), we need to approximate $Z[Z_m^{-1}F_h]$ and $Z[Z_s^{-1}F_e]$ by products of $F_h(z)$ and $F_e(z)$ given that Z_m^{-1} and Z_s^{-1} are double integrators.

Two Taylor series expansions of $g(t) = \int_0^t \int_0^r f(r) dr ds$ around the sampling instant kT are

$$\begin{aligned} g(kT \pm T) &= g(kT) \pm Tg'(kT) + (T^2/2)g''(kT) \\ &\quad \pm (T^3/6)g'''(kT) + O(T^4). \end{aligned} \quad (10)$$

Since $g''(kT) = f(kT)$, summing $g(kT+T)$ and $g(kT-T)$ and taking Z transform on both sides gives the Verlet double integrator

$$G(z) = T^2 \frac{z}{(z-1)^2} F(z) = V_3(z) F(z), \quad (11)$$

which is an order more accurate than integration by the Euler method as third-order terms in the Taylor expansions cancel out. The double integration precision can be increased to $O(T^6)$ where fifth-order terms cancel out – for details, see [5].

On the basis of (11),

$$Z[Z_{m,s}^{-1} F_{h,e}] = \frac{V_3(z)}{M_{m,s}} F_{h,e}(z). \quad (12)$$

Replacing (8) and (11) in (7) gives the hybrid model of the digitally controlled teleoperation system as

$$\begin{bmatrix} F_h(z) \\ -X_s(z) \end{bmatrix} = \begin{bmatrix} h_{11}(z) & h_{12}(z) \\ h_{21}(z) & h_{22}(z) \end{bmatrix} \begin{bmatrix} X_m(z) \\ F_e(z) \end{bmatrix}. \quad (13)$$

4 Experimental results

4.1 Experimental setup

This section presents our experimental setup and the differences between the two cases of discrete-time and continuous-time control in terms of hybrid matrices. In both cases, the teleoperation system consists of two identical Servo SRV-02 Quick Connect Modules (Quanser Inc., Markham, ON, Canada) as 1-degree-of freedom revolute-joint master and slave robots (Fig. 3). Each of the master and slave modules, which is comprised of a DC motor, a gear, and a potentiometer, is preceded by an inner current control loop so that an outer position control loop can send torque commands (i.e., F_m and F_s in Fig. 2) to each robot. While the current control loop is always implemented by analog components, the position controller can be implemented either in the continuous-time or the discrete-time domain.

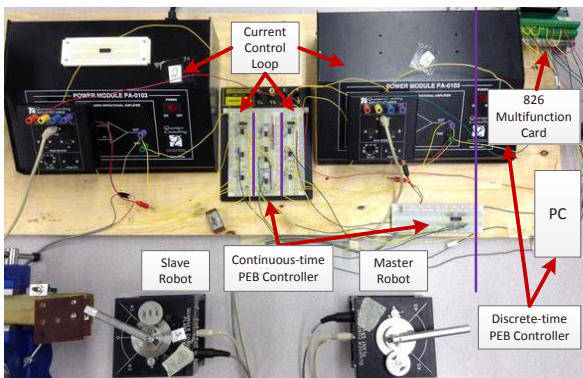


Fig. 3.

The experimental setup of bilateral teleoperation system

The continuous-time absolute stability criterion used here was proposed by Llewellyn for two-port networks [6]: The PEB teleoperation system of Fig. 1 is absolutely stable if $k_{pm}, k_{vm}, k_{ps}, k_{vs} > 0$ and $C_m(s)/C_s(s) = \alpha$, where α is a positive constant.

For the discrete-time stability, after the PD controllers are discretized, a sufficient stability condition can be found for the sampled-data teleoperator [3] as

$$\frac{b_m b_s}{b_s + b_m} > \frac{k_p T}{2} + k_v, \quad (14)$$

where $k_{vm} = k_{vs} = k_v$, and $k_{pm} = k_{ps} = k_p$, for a given teleoperation system, the left side of (14) is fixed. Thus, the stability condition puts an upper bound on $k_p T$ and k_v .

4.2 Parameter h_{11}

In our experiment, if the master's and/or the slave's positions become unbounded or oscillate indefinitely, the teleoperation system is judged to be unstable. As explained in Section 2, the hybrid parameter $h_{11} = F_h/sX_m|_{F_e=0}$ is the input impedance felt by the operator in the free-motion condition. The smallest sampling period (i.e., the largest sampling rate) achievable in our system is 1 millisecond (ms), which is used in the following experiments.

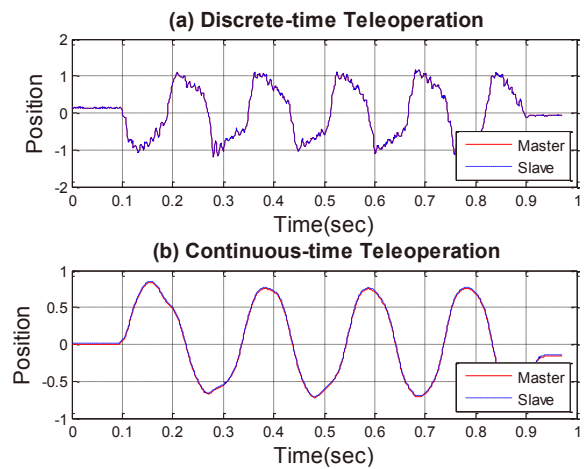


Fig. 4: Comparison of the master-slave position tracking profiles in two teleoperation systems when the operator moves the master and the slave is in free space.

In Fig. 4, the proportional controller gains are 20 for (a) and 80 for (b), which are the maximum gains that can be obtained in the discrete-time controlled system and the continuous-time controlled system, respectively under the stability conditions (14). The Euclidean norms of the position tracking errors are 0.0686, 0.0625 for (a) and (b), respectively. There should be no theoretical upper bound on the continuous-time control gain for stability, however, the gain is limited by issues like measurement noise and saturations of the op-amps.

It can be seen from Fig. 4 that in both the continuous-time haptic teleoperation system and the discrete-time teleoperation system, free motion task can be accomplished easily with small position tracking errors, which indicate there is no obvious difference of h_{11} between the two kinds of control. This is not the case, however, for the other three parameters h_{12} , h_{21} and h_{22} as seen below.

4.3 Parameters (h_{12} , h_{21} , h_{22})

1) *Mathematical Comparisons between the Discrete-time Controlled and Continuous-time Controlled Teleoperation Systems*

In this section, the hybrid parameters are derived and analyzed using the mathematical tool Maple (Maplesoft, Waterloo, ON CA), in order to see whether we can mathematically verify there is a better transparency performance in the continuous-time teleoperation system than in its discrete-time counterpart.

We compare the absolute values of h_{12_DT}/h_{12_CT} , h_{21_DT}/h_{21_CT} and h_{22_DT}/h_{22_CT} , where DT indicates the parameters in the discrete-time controlled teleoperator and CT indicates the parameters in the continuous-time controlled teleoperator. The results are shown in Fig. 5. The four different discrete-time control gains used here are the maximum gains achievable under the corresponding sampling periods.

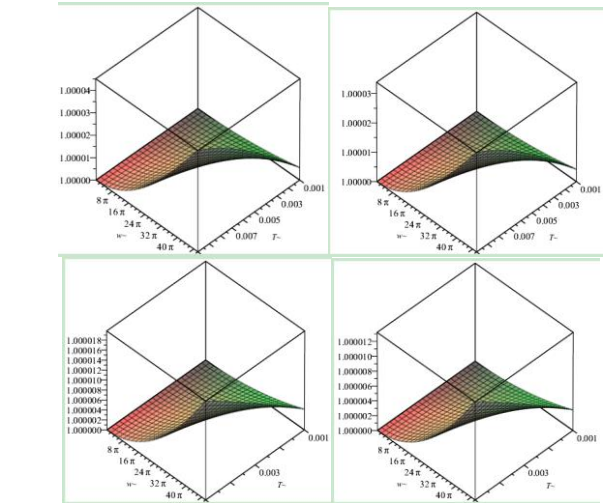
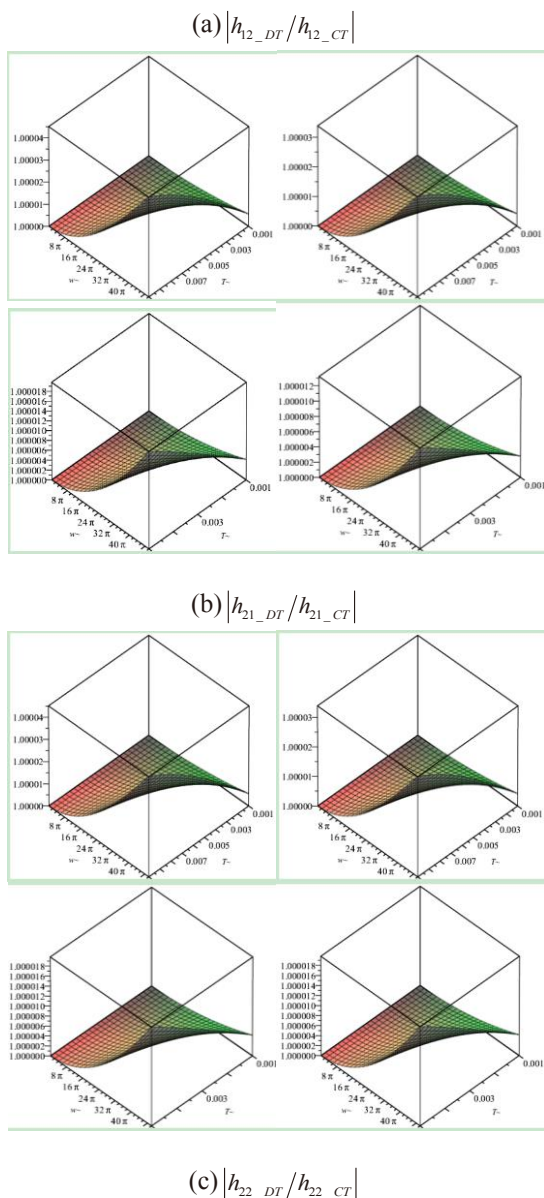


Fig. 5. Mathematical comparison between the discrete-time controlled and continuous-time controlled teleoperation systems. Each group ((a) to (c)) contains four graphs, which correspond to discrete-time control with different gains. For the continuous-time controller, the maximum control gain 80 obtained in Section 4.1 is used in all cases. The discrete-time control gain is 15 in the top left plot for both the master and the slave, is 15 for the master and 20 for the slave in the top right plot, is 20 for both robots in the lower left plot, and is 20 for the master and 30 for the slave in the lower right plot.

As shown in Fig. 5, the ratios of the absolute values of the hybrid parameters of the discrete-time controlled system to the continuous-time teleoperation system are all larger than 1. This means that as the sampling period changes and as the frequency changes, the performance of the discrete-time controlled teleoperator changes. In other words, unlike the continuous-time controlled case, the performance of the discrete-time controlled teleoperator is sensitive to the sampling period.

It is evident that for the three hybrid parameters, we get bigger differences between the discrete-time controller and the continuous-time controller as the frequency increases and as the sampling rate decreases. It means under any fixed frequency, we can obtain better performance (closer to the performance of the continuous-time system) as the sampling period gets smaller. However, due to the trade-off between the sampling period and the proportional gain of the PD controllers in stability conditions (14), we cannot always get small enough sampling period under the corresponding maximum control gain, which means the discrete-time controlled teleoperation system cannot achieve the good transparency the continuous-time controlled teleoperation system can attain. This is a mathematical validation of better transparency of the continuous-time controlled teleoperation. Next, we will see whether the experimental results are in accordance with these mathematical results.

2) Experimental Comparisons between the Discrete-time Controlled and Continuous-time Teleoperation System

Two different kinds of tests have been performed to find the hybrid parameters. First, in free-motion tests, a human operator moves the master robot back and forth for about 1 minute while the slave robot moves in free space. Since $F_e = 0$, the frequency responses $h_{11} = -X_s/X_m$ can be found by applying spectral analysis (MATLAB function *spa*)

on the free-motion test data. Second, other tests are done by fixing the master robot to a wall while trying to move the slave robot by applying forces on it. Since $X_m = 0$, the frequency responses $h_{12} = F_h/F_e$ and $h_{22} = -sX_s/F_e$ can be found. In the above two tests, the force data concerning external interactions of master robot and slave robots are recorded by two JR3 (JR3 Inc., Woodland, CA 95776 USA) force sensors. The largest control gains for the two teleoperation systems under stable conditions were obtained from Section 4.1 and used in the two tests; this is a gain of 20 for the discrete-time controlled system with 1 millisecond sampling period, and 80 for the continuous-time controlled system.

The magnitudes of the hybrid parameters of the two teleoperation systems are shown in Fig. 6. As can be seen in Fig. 6, the continuous-time controlled teleoperation system shows its superiority in terms of transparent performance considering the ideal transparency requirement (5).

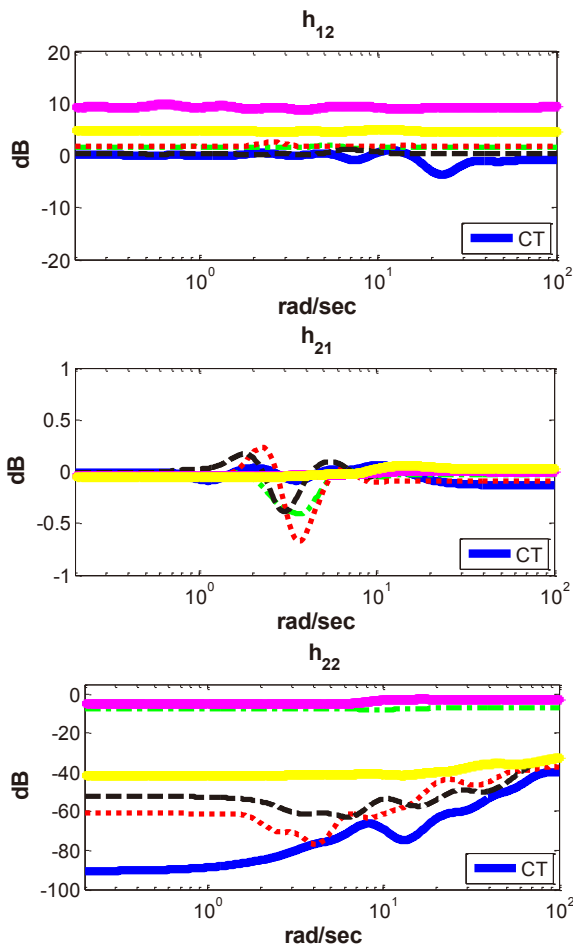


Fig. 6. Magnitudes of the hybrid parameters for the teleoperation systems: (solid, blue) continuous-time teleoperation system, others are discrete-time controlled system with different control gains and sampling periods: (-, green) control gain is 20 for both robots with 1 ms sampling period; (:, red) control gain is 15 for both the master robot and the slave robot with 1 ms sampling period; (--, black) control gain is 20 for the master robot and 30 for the slave robot with 1 ms sampling period; (solid, magenta) control gain is 20 for both robots with 1 ms sampling period; (solid, yellow) control gain is 20 for the master robot and 30 for the slave robot with 1 ms sampling period.

The better force tracking performance of the continuous-time teleoperation system, i.e., $h_{12} \approx 0 \text{ dB}$, demonstrates a better force tracking performance for the continuous-time teleoperation system. With regard to h_{21} , most spectra are close to 0 dB with the continuous-time controlled system having a more consistent performance across different frequencies. With regard to h_{22} , the values are closer to the idea value for the continuous-time controlled system. Overall, these results are consistent with the mathematical results and they demonstrate that a continuous-time controller can significantly increase the teleoperator transparency without sacrificing the stability of the teleoperation system. This included an experimental validation of better transparency of the continuous-time controlled teleoperation system.

5 Conclusions and Future Work

In this article, we showed that a continuous-time controller can achieve better transparency comparing to its discretized counterpart. Possible extensions of the current study include designing hybrid continuous-time and discrete-time controllers for teleoperation systems to benefit from the better transparency characteristics of the former and the flexibility of the latter.

References

- [1] K. Ogata, Discrete-time control systems, 2nd Edition: Prentice Hall, 1995.
- [2] F. J. Sharifi and I. Hassanzadeh, "Experimental analysis of mobile-robot teleoperation via shared impedance control," *IEEE Trans. on Systems, Man, and Cybernetics-Part B: Cybernetics*, vol. 41, no. 2, pp. 591-606, 2011.
- [3] A. Jazayeri and M. Tavakoli, "Absolute Stability Analysis of Sampled-data scaled bilateral teleoperation systems," *Control Engineering Practice*, 21: 1053-1064, 2013.
- [4] A. Jazayeri and M. Tavakoli, "Stability analysis of sampled-data teleoperation systems," 49th *IEEE Conf. on Decision and Control (CDC)*, 2010: 6.
- [5] M. Tavakoli, A. Aziminejad, "Discrete-time bilateral teleoperation: modelling and stability analysis," *IET Control Theory and Applications*, vol. 2, no. 6, pp. 496-512, 2008.
- [6] F. B. Llewellyn, "Some fundamental properties of transmission systems," *Proc. of the Institute of Radio Engineers*, vol. 40, pp. 271-283, 1952.